Structural and spectroscopic investigations of CdS/HgS/CdS quantum-dot quantum wells

A. Mews, A. V. Kadavanich, U. Banin, and A. P. Alivisatos
Department of Chemistry, University of California, Berkeley, California 94720
and Materials Sciences Division, Lawrence Berkeley National Laboratory, University of California, Berkeley, California 94720
(Received 29 January 1996)

Epitaxial growth in a CdS/HgS heterostructure of nanometer dimensions, prepared by methods of wet chemistry, is demonstrated. High-resolution transmission-electron microscopy is used to determine the shape and crystallinity of this system consisting of a quantum well in a quantum dot. The homogeneous absorption and fluorescence spectra are investigated by transient hole burning and fluorescence line-narrowing spectroscopy. The photophysical measurements provide evidence for charge-carrier localization within the HgS well. [S0163-1829(96)51420-7]

The electronic and structural properties of semiconductor nanocrystals have been intensively studied within the last 15 years.[1,2] The still increasing interest in this class of material is due to the size-dependent optical properties in the regime where the nanocrystal is smaller than the bulk exciton. As the size of the nanocrystal is decreased, quantum confinement of the charge carriers causes a blueshift of the absorption onset of up to 1 eV and the development of discrete features in the optical spectra.

The size dependence of the physical properties of nanocrystals has been studied in high-quality samples, which can be prepared by colloidal solution chemistry. With such methods it is possible to prepare nanocrystals, e.g., CdS and CdSe, of any diameter between 2 and 10 nm with less than 5% size distribution.[3,4] In these samples the nanocrystal surface is covered with organic ligands, which make the particles soluble and prevent aggregation. These particles can also be used as building blocks for more complex structures such as superlattices.[5,6] They have also been used in electronic devices such as light-emitting diodes (LED's).[7,8]

This chemical flexibility comes at the expense of surface passivation. The large organic molecules used to make the particles soluble do not match the close packing of the inorganic atoms on the nanocrystal surface. This leaves some surface sites unsaturated, which can lead to trapping of charge carriers on surface dangling bonds. In planar structures such as quantum wells, epitaxial growth of one semiconductor on top of another is used to passivate these surface states. Recent theoretical work suggests that it is possible to create analogous structures in quantum dots, using concentric shells of alternating materials to build up a confinement potential.[9]

Weller and co-workers have used colloidal chemistry techniques to prepare samples in which a shell of HgS ($E_{gap}=0.5$ eV) is embedded in a CdS ($E_{gap}=2.5$ eV) quantum dot[10] (Fig. 2, inset), forming a ''quantum-dot quantum well'' (QDQW). Analogous to planar quantum wells, the strong confinement of the charge carriers within the embedded HgS region should lead to well-separated electronic states that are not influenced by surface effects. Previously, chemical evidence had been used to argue that the expected CdS/HgS/CdS shell structure was produced, but the detailed morphology and electronic structure have yet to be determined.

In this paper we first use high-resolution transmission-electron microscopy (HRTEM) to investigate the structure of these particles. The results show that epitaxial growth of quantum wells in nanocrystals does indeed occur, provided the crystallites have well-defined faceted shapes to begin with. We then present size selective absorption and fluorescence spectra measured by transient hole burning and fluorescence line-narrowing spectroscopy to demonstrate that the electronic excitation is concentrated in the shell of HgS.

The synthesis of the QDQW's is described in detail elsewhere.[10] The first step is the preparation of the CdS cores by reaction of a cadmium salt with H_2S in aqueous solution. A typical HRTEM micrograph of a CdS nanocrystal [Fig. 1(a2)], shows a triangular feature against the speckled background arising from the amorphous carbon substrate. The spacings and angles between lattice lanes show that the nanocrystal is aligned along the (110) axis of the zinc-blende crystal structure of CdS. The decrease of contrast in going from the apex to the base implies a decrease in thickness. This suggests that the nanocrystal is a tetrahedron terminated in (111) surfaces [Fig. 1(a1)]. This shape represents a natural Wulff polyhedron[11] in which only (111) surfaces, either cadmium or sulfur terminated, are present. Since anionic polyphosphate ligands are at the surfaces of the nanocrystals, the best explanation for the observed morphology is to assume that the exposed surfaces are cadmium rich, as illustrated. The corresponding HRTEM simulation[12] [Fig. 1(a3)] agrees with this interpretation of the experimental image, but only a small fraction of the crystallites are aligned along the proper crystallographic axis to allow the shape to be discerned. 75% of that fraction showed the triangular projection with (111) surfaces and a mean edge length of 50 Å (+/−17%). The remaining structures can be assigned to truncated octahedra and heavily faulted crystals.

The basic morphology is preserved in the next step of the synthesis, in which the surface cadmium ions of the CdS crystallites are exchanged with mercury. This can be done by addition of mercury ions to the solution because HgS has a lower solubility than CdS. Figure 1(b) shows a model of the structure resulting from single monolayer substitution. Within the statistical error, the mean size and size distribution is unchanged. However, defect structures become more prevalent and 64% of the oriented particles have tetrahedral shape.

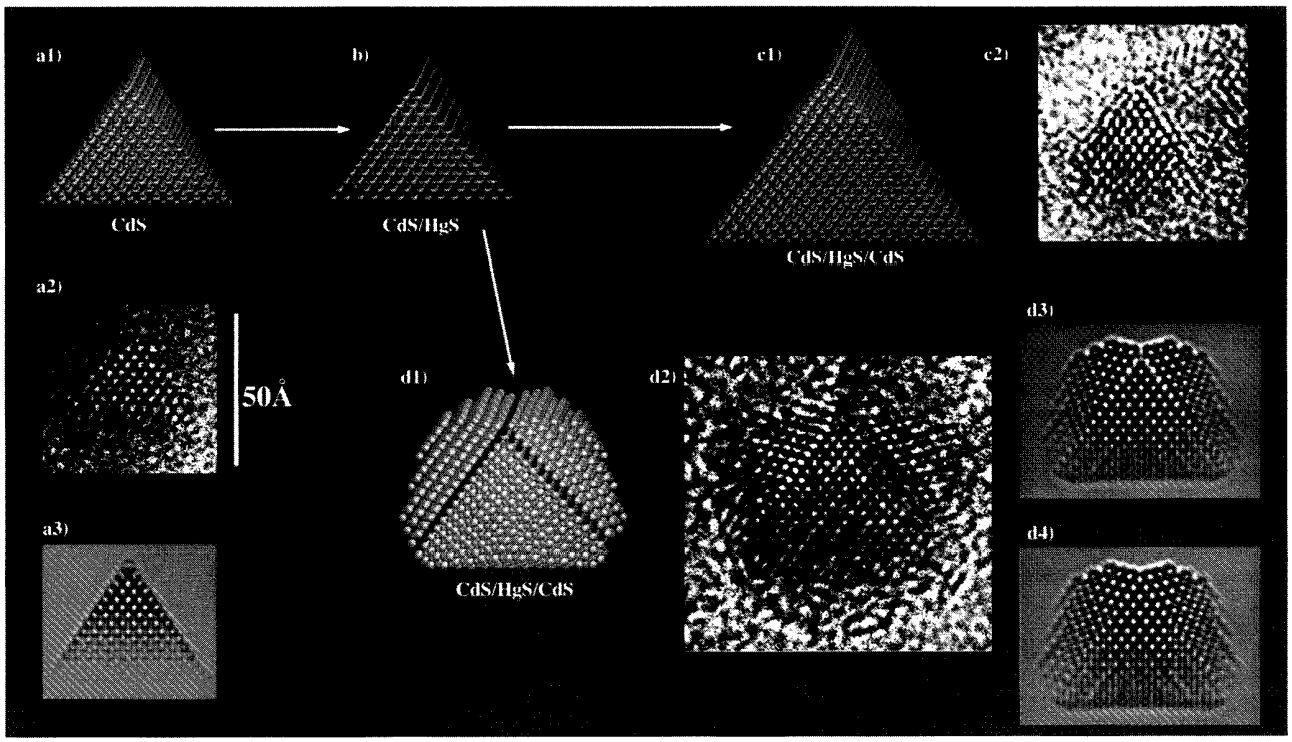

FIG. 1. HRTEM study of the structural evolution of the CdS/HgS/CdS nanostructure. The micrograph of a CdS core cluster (a2), exhibits tetrahedral morphology, which is in agreement with the TEM simulation (a3). The corresponding molecular model (a1) shows that all surfaces are cadmium terminated (111). (b) shows a model of the CdS particle after surface modification with Hg. A typical micrograph of a tetrahedral CdS/HgS/CdS nanocrystal is shown in (c2) along with a corresponding model (c1). Model (d1) and micrograph (d2) represent a CdS/HgS/CdS nanocrystal after twinned epitaxial growth. The arrow marks the interfacial layer exhibiting increased contrast due to the presence of HgS, in agreement with the simulation (d3). No contrast change is seen in a simulation of a model with all Hg replaced by Cd (d4).

The final coating of these particles is carried out by adding excess cadmium ions to the solution and growing CdS on top of the HgS layer via slow H_2S injection. This reaction takes place at pH 5.5, where the chemical equilibria are such that nucleation of new CdS particles is suppressed. 63% of the resulting nanocrystals show tetrahedral shape [Fig. 1(c)]. The average size increases to 62 Å ($+/-24\%$) edge length. Furthermore, no ''amorphous region'' can be detected in any of the micrographs, suggesting epitaxial growth of the layers. The close match of the CdS and HgS lattice parameters ($a_{\mathrm{HgS}}=5.852$ Å , $a_{\mathrm{CdS}}=5.818$ Å)[13] and the presence of faceted crystallites with only one exposed plane favor this growth mode.

Half of the nontetrahedral nanocrystals show a different structure similar to that in Fig. 1(d). Here twin faults on the tetrahedral surfaces have resulted in the final CdS layers growing out of phase with the core. This arises by introducing one layer of hexagonal (wurtzite) stacking into an otherwise cubic (zinc-blende) structure and does not lead to a loss of passivation, as no bonds are broken. The cap layers on adjacent faces are crystallographically mismatched and cannot grow into each other. A model for this structure is shown in Fig. 1(d1). When viewed along the (110) crystallographic axis, two of the HgS planes are viewed edge-on and the initial CdS core can clearly be seen as a triangle. Close inspection of the micrograph shows a line of enhanced contrast along the twin fault [Fig. 1(d2), arrow] corresponding to the higher contrast of mercury relative to cadmium. The contrast change is reproduced in the simulation of the HRTEM image [Fig. 1(d3)], while the same model with cadmium in place of the mercury shows no such contrast change [Fig. 1(d4)]. The simulation for the tetrahedral model [Fig. 1(c)] shows a mild contrast change, but it is undetectable above background noise in the experiment.

These structural studies demonstrate that the low band-gap HgS layer is epitaxially embedded in the larger gap CdS. Quantum confinement requires that the corresponding optical spectrum will exhibit discrete structure with a threshold higher in energy than the bulk HgS band gap of 0.5 eV. The evolution of the inhomogeneous absorption spectrum during the course of preparation is shown in Fig. 2 (top). The initial CdS core particles [Fig. 1(a)] are comparable to the bulk exciton dimension (diameter $=50$ Å)[13] and exhibit little quantum confinement from the bulk band gap of 2.5 eV. When the surface CdS is replaced by HgS the spectrum [Fig. 1(b)] shifts red of the bulk CdS gap. The final CdS ''capping'' leads to a further redshift in the absorption spectrum of 0.5 eV [Fig. 1(c)]. Note that the growth of surface CdS, whose bulk band gap is 2.5 eV, leads to a decrease of the first electronic transition to approximately 2 eV. This can only be observed in systems with low dimensionality in which the confinement effect is reduced by an enlargement of the system.[9] Furthermore, the nanocrystals show luminescence (Fig. 2, *c*) with quantum yields of several percent at room temperature. This is a direct result of the surface passivation because the outermost CdS ''cap'' eliminates non-

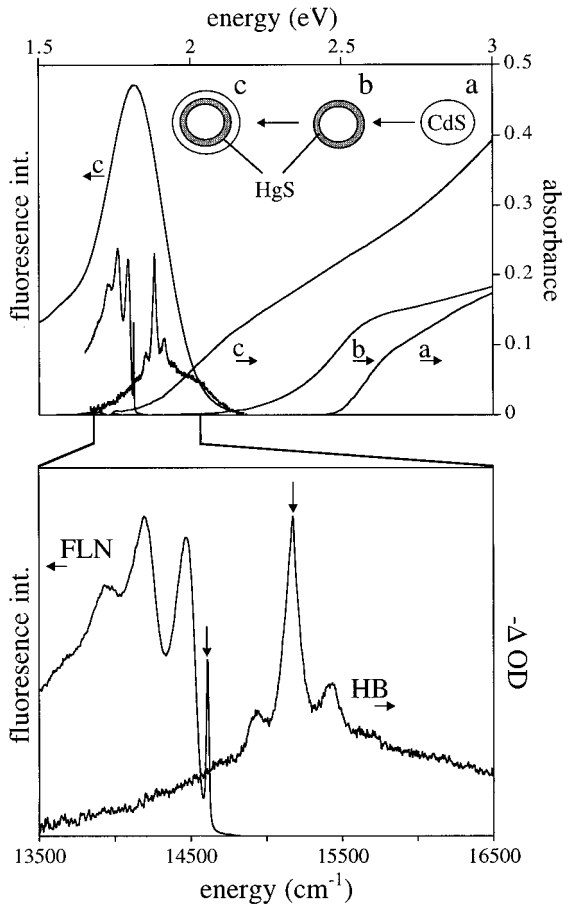

FIG. 2. Top: Evolution of the inhomogeneous absorption spectra during the synthesis. The HgS-covered particles (b), exhibit a redshift relative to the CdS core particles (a). The absorption (c) and emission spectra (γ_{ex}=514 nm) of the final CdS/HgS/CdS are also shown. Bottom: FLN and HB spectra at the red edge of the inhomogeneous absorption of the CdS/HgS/CdS structure with arrows marking the excitation energy. In the FLN spectrum (left spectrum) some of the laser light was detected, indicating the Stokes shift between the excitation and the zero-phonon line. The HB spectrum (right) shows a narrow resonant hole centered at the excitation energy and well-resolved phonon side bands with the frequency of the bulk LO phonon of HgS (250 cm^{-1}).

radiative surface traps from the HgS layer recombination region. Thus the complete heterostructure exhibits spectral features at the expected energy but does not show the discrete structure required by quantum confinement. As we demonstrate below, the broadening is due to variations in size and morphology of the CdS/HgS/CdS crystallites in the sample. Using hole burning (HB) and fluorescence line-narrowing (FLN) spectroscopy, we have investigated the homogeneous (''single particle'') optical properties for absorption and emission and these do display the expected optical features.

In the transient HB experiment, excitation by a nanosecond pump pulse depopulates the ground state of a distinct ''homogeneous'' set of particles.[14,15] The missing transitions appear as a bleach in the absorption spectrum (a spectral hole) recorded a few nanoseconds later with a spectrally broad probe beam. The HB spectrum of Fig. 2 shows a narrow band centered at the pump energy, which is associated with particles having the first electronic transition at the excitation frequency. The homogeneous linewidth of 55 cm^{-1} (7 meV) is a small fraction of the width of the inhomogeneous absorption spectrum and is comparable to other colloidal nanocrystals of the same size. This supports a model in which the linewidth is not related to surface effects but can be explained by a coupling of the electronic transition to low-frequency acoustic modes. In this model the homogeneous linewidth shows a strong size dependence ($1/R^5$) which leads to the observed broadening in this size regime.[16,17]

In addition to the resonant line, vibrational side bands are resolved in the HB spectra. The appearance of the side bands reflects the strong coupling of the electronic excitation to LO phonons, which results from the distortion of the ionic lattice upon the alteration of the charge distribution in the sample. The observed vibrational frequency of 250 cm^{-1} is identical to the bulk LO mode of HgS (253 cm^{-1})[18] and much lower than the CdS LO frequency (300 cm^{-1}).[13] Phonon confinement may lead to a small redshift of the LO mode. However, as the redshift is only a few cm^{-1}, the observed phonon is consistent with a HgS-like mode.[19] In nanocrystal alloys, Raman studies show the existence of two modes with frequencies close to those of the pure compounds, and intensity ratios proportional to the composition.[20] In our case, a single HgS-like mode is observed, despite the fact that the Hg cation fraction is only 20%. This supports a picture of localized excitation in the thin HgS layer, coupling to the HgS-like mode. In quantum wells grown by molecular-beam epitaxy, Raman measurements exhibit a vibrational fine structure assigned to various LO and interfacial vibrational modes.[21] In our HB experiment, the intrinsic broadening of the absorption line does not allow resolution of additional modes. Raman measurements in these structures as well as theoretical studies of the electron-vibrational coupling will be useful in understanding the extent of charge-carrier localization.

The phonon progression is also observed in the FLN experiment. FLN achieves optical selection by tuning the laser wavelength to the red part of the inhomogeneous absorption spectrum, thus exciting a small subset of crystallites[22] (see Fig. 2). We extract a 255-cm^{-1} LO phonon mode for the first two peaks, which varies to slightly lower frequencies for higher vibrational levels. This result suggests that not only the absorption, but also the radiative recombination of electrons and holes takes place centered in the HgS well region. An additional interesting feature of the FLN spectra is the appearance of a 150-cm^{-1} (19 meV) shift between the excitation frequency and the first emission-peak position. This ''Stokes shift,'' which has also been observed in other nanocrystal systems, can be explained by assuming that the emitting state is different from the absorbing state. In this inorganically passivated system, the relatively large Stokes shift may support a model in which this is not related to surface effects but is rather an intrinsic property of semiconductor nanocrystals.[23] The CdS cap layer is still thin, however, and the possibility still exists for mixing with surface states, which act as traps for the charge carriers.[24]

In summary, the HRTEM data and the homogeneous optical measurements demonstrate the existence of epitaxially grown nanocrystals fabricated by wet chemical

methods. The realization of a potential well within a quantum dot allows one to manipulate the electronic properties by variation of the CdS core, the HgS shell, and the outer CdS layers. Naturally, this leads to additional sources of inhomogeneity, in particular, slight variations in the HgS layer thickness will cause substantial spectral shifts. An additional source of inhomogeneity is possible variations in the morphology. However, the homogeneous photophysical measurements have shown that the intrinsic electronic properties of colloidal semiconductor nanocrystals can be altered by the formation of complex heterostructures. These results suggest that the advanced concepts for tailoring materials developed for planar structures can also be applied to lower-dimensional systems, in a way that is compatible with wet chemistry.

The authors acknowledge the support of the ONR/Berkeley National Lab Molecular Design Institute. The TEM's were collected at the National Center for Electron Microscopy. A.M. thanks the Deutsche Forschungsgemeinschaft (DFG) for financial support. U.B. thanks the Fulbright Foundation for financial support. We acknowledge useful discussions with Dr. S. H. Tolbert and Dr. N. C. Greenham.

[1] L. E. Brus, IEEE J. Quantum Electron. **22**, 1909 (1986).
[2] A. Henglein, Top. Curr. Chem. **143**, 115 (1988).
[3] C. B. Murray, D. B. Norris, and M. G. Bawendi, J. Am. Chem. Soc. **115**, 8706 (1993).
[4] T. Vossmeyer *et al.*, J. Phys. Chem. **98**, 7665 (1994).
[5] T. Vossmeyer *et al.*, Science **267**, 1476 (1995).
[6] C. B. Murray, C. R. Kagan, and M. G. Bawendi, Science **270**, 1335 (1995).
[7] V. L. Colvin, M. C. Schlamp, and A. P. Alivisatos, Nature **370**, 354 (1994).
[8] B. O. Dabboussi *et al.*, Appl. Phys. Lett. **66**, 1316 (1995).
[9] D. Schooss, A. Mews, A. Eychmueller, and H. Weller, Phys. Rev. B **49**, 17 027 (1994).
[10] A. Mews *et al.*, J. Phys. Chem. **98**, 4109 (1994).
[11] G. Wulff, Z. Kristallogr. **34**, 449 (1901).
[12] We used Biosym's Insight II software package for TEM micrograph simulations, which employs the multislice algorithm of Goodman, Moodie, and Cowley: J. M. Cowley and A. F. Moodie, Acta Cryst. **10**, 609 (1957); P. Goodman and A. F. Moodie, Acta Cryst. **A30**, 280 (1974).
[13] I. Broser, R. Broser, and M. Rosenzweig, in *Numerical Data and Functional Relationships in Science & Technology*, edited by D. Madelung, Landolt-Börnstein, New Series, Group III, Vol. 17, Pt. b (Springer-Verlag, Berlin, 1982).
[14] A. P. Alivisatos *et al.*, J. Chem. Phys. **88**, 4001 (1988).
[15] D. J. Norris, A. Sacra, C. B. Murray, and M. G. Bawendi, Phys. Rev. Lett. **72**, 2612 (1994).
[16] D. M. Mittleman *et al.*, Phys. Rev. B **49**, 14 453 (1994).
[17] U. Banin, G. Cerullo, and A. A. Guzelian (unpublished).
[18] W. Szuszkiewicz, B. Witkowska, and M. Jouanne, Acta Phys. Pol. **87**, 415 (1995).
[19] J. J. Shiang, S. H. Risbud, and A. P. Alivisatos, J. Chem. Phys. **98**, 8432 (1993).
[20] A. Tu and D. Persans, Appl. Phys. Lett. **58**, 1506 (1991).
[21] K. T. Tsen, K. R. Wald, T. Ruf, P. Y. Yu, and H. Morkocced, Phys. Rev. Lett. **67**, 2557 (1991).
[22] M. Nirmal, D. J. Norris, M. Kuno, M. G. Bawendi, Al Efros, and M. Rosen, Phys. Rev. Lett. **75**, 3728 (1995).
[23] Al. A. Efros and A. V. Rodina, Phys. Rev. B **47**, 10 005 (1993).
[24] M. G. Bawendi *et al.*, Phys. Rev. Lett. **65**, 1623 (1990).